

Article

Multi-Period Transmission Expansion Planning for Renewables-Rich Power Grid Enabling Transfer Capacity Enhancement of Hybrid AC/DC Interface [†]

Li Shen ¹, Li Jiang ¹, Qing Wang ¹, Yiyu Wen ¹ and Tingjian Liu ^{2,*}¹ State Grid Southwest Branch Corporation, State Grid Corporation of China, Chengdu 610095, China² College of Electrical Engineering, Sichuan University, Chengdu 610065, China

* Correspondence: liutj@scu.edu.cn; Tel.: +86-151-9661-1260

[†] This paper is an extended version of our paper published in 2022 4th International Conference on Electrical Engineering and Control Technologies (CEEET), Shanghai, China, 16–18 December 2022, pp. 396–400.

Abstract: With the increasing integration of HVDC tie-lines, the regional power systems in both the energy-exporting area and the energy-importing area have been gradually evolving into “strong DC, weak AC” systems. In this paper, a multi-period transmission expansion planning optimization model is proposed for an energy-exporting power grid with hybrid AC/DC interface. While the existing literature has not considered the dynamic security problem in TEP, this paper adopts the conventional total transfer capacity (TTC) index to evaluate the security limit of hybrid AC/DC interface under different transmission expansion schemes. Multiple objectives are considered to reduce the investment cost while promoting the consumption of renewables by enhancing the total transfer capacity of hybrid AC/DC interface. The non-dominated sorting genetic algorithm-II (NSGA-II) is used to compute the optimal solution for the proposed multi-period multi-objective transmission expansion planning problem. A case study on the modified IEEE 39-bus system is presented to demonstrate the effectiveness of the proposed method.

Keywords: transmission expansion planning; multi-period planning; renewables-rich power grid; hybrid AC/DC interface; transfer capacity



Citation: Shen, L.; Jiang, L.; Wang, Q.; Wen, Y.; Liu, T. Multi-Period Transmission Expansion Planning for Renewables-Rich Power Grid Enabling Transfer Capacity Enhancement of Hybrid AC/DC Interface. *Energies* **2023**, *16*, 2170. <https://doi.org/10.3390/en16052170>

Academic Editor: Alon Kuperman

Received: 29 December 2022

Revised: 12 February 2023

Accepted: 21 February 2023

Published: 23 February 2023



Copyright: © 2023 by the authors. Licensee MDPI, Basel, Switzerland. This article is an open access article distributed under the terms and conditions of the Creative Commons Attribution (CC BY) license (<https://creativecommons.org/licenses/by/4.0/>).

1. Introduction

The increase in electricity demand and the advocacy of emission reduction together raise the need for promoting the integration and consumption of renewable energy sources (RES). However, RES, such as hydro power, wind power and photovoltaic power, are usually located far from the load center. Take China as an example: RES locates on the western region while the load centers are on the eastern region. To this end, high-voltage direct-current (HVDC) transmission systems are being developed for global energy efficiency. In comparison with conventional high-voltage alternative-current (HVAC) tie-lines, HVDC systems have some attractive benefits, such as less economical investment and asynchronous interconnection of AC power systems [1]. However, with the increase in power transmitted by these HVDC tie-lines, the regional power grids at both ends, i.e., the energy-exporting area and energy-importing area, have been gradually evolving into “strong DC, weak AC” systems [2]. These characteristics of “strong DC, weak AC” means that, when subjected to disturbances such as HVDC commutation failures (CFs) or HVDC blocking, the power grid will lose its stability, which inevitably results in catastrophic outages. To address this problem, the transmitted power through either the HVDC tie-lines or the AC tie-lines need to be reduced in the compromised manner for power system security consideration. Although there are a handful of projects that study the stability mechanism [3] and the controlling strategy [4,5] for protecting the hybrid AC/DC power system from insecurity, the reinforcement of the AC power grid is more important as

it is essential for supporting the secure operation of the hybrid AC/DC power systems. In other words, if the AC power grids is not reinforced, the transferring power of the HVDC tie-lines has to be reduced, aiming at preventing the instability of the AC power system, which inevitably lead to the curtailment of RES and/or the operating efficiency of the hybrid power system.

Network reinforcement is usually referred to as transmission expansion planning (TEP). Transmission expansion planning (TEP) is widely studied for network reinforcement and to accommodate the increasing integration of supply and demand. In terms of transmission expansion planning, numerous studies in the literature on transmission expansion planning of AC power network have been reported. However, few studies have investigated the TEP of hybrid AC\DC transmission networks. For receiving-end power systems, the exceeding short-circuit current and multi-infeed DC interaction are of concern. An NSGA-II-based optimization method is proposed in [6] to coordinate these two problems. In [7], A hybrid ac/dc transmission expansion planning model is proposed to minimize the total investment, operation and load shedding costs, and the Benders decomposition approach is used to solve the TEP problem. In [8], the continuously variable series reactor (CSVSR) is introduced to TEP problem and with properly allocated CSVSRs, the planning costs of the TEP problem can be reduced as the CSVSRs can be used to enable the flexible regulation of power flow to deal with N-1 contingencies. In [9], the conversion of existing HVAC transmission lines to HVDC lines is considered in a multi-year TEP model and this conversion can reduce the investment cost while increasing the transfer capability to accommodate the integration of remote renewables resources. In [10], a multi-period hybrid AC/DC network expansion planning model that incorporates node voltages, reactive power and network losses is proposed and a second-order conic relaxation is proposed to cope with this complex non-convex problem. In [11], a multi-stage robust TEP model is proposed to reinforce the sending-end power system in order to withstand the conventional HVAC N-1 contingencies and the HVDC bi-pole blocking contingencies. In [12], apart from TEP, a multi-period integrated framework is proposed for coordinated generation expansion planning (GEP), TEP and natural gas grid expansion planning (NGGEP). However, none of the above mentioned studies in the literature consider the dynamic security problem of the hybrid AC/DC power grid. Previously, the authors have proposed a bi-level TEP model in [13]. In this model, the dynamic security of the planned AC/DC transmission network is assessed in the lower-level, but this model is limited to single-stage expansion planning.

In this paper, a multi-period transmission expansion planning optimization model is proposed for the energy-exporting area with hybrid AC/DC interface. The major contributions of this paper are as follows:

- (1) While the existing literature has not considered the dynamic security problem in multi-stage TEP, we use the total transfer capacity (TTC) index to evaluate the dynamic security limit of hybrid AC/DC interface under different transmission expansion schemes;
- (2) Multiple objectives are considered to reduce the investment cost while promoting the consumption of renewables by enhancing the total transfer capacity of hybrid AC/DC interface.

Case study on the modified IEEE 39-bus system is presented to demonstrate the effectiveness of the proposed method.

The rest of this paper is organized as follows. In Section 2, the mathematical modeling of the transfer capacity of hybrid AC/DC interface is discussed and then a heuristic method is proposed to compute the transfer capacity. In Section 3, a multi-period transmission expansion planning optimization model is proposed for an energy-exporting power grid with hybrid AC/DC interface. In Section 4, case study is presented to demonstrate the effectiveness of the proposed method. Finally, a conclusion is made in Section 5.

2. Transfer Capacity of Hybrid AC/DC Interface

Figure 1 depicts the renewable-rich power grid with hybrid AC/DC transmission interface. Renewable generations, such as wind power, photovoltaic power and hydro power, are located in the remote and energy-exporting area where the regional load demand is comparatively low. To promote the consumption of these renewables, the redundant generations are transferred via the HVDC tie-lines and the AC tie-lines to the load center in the energy-importing area.

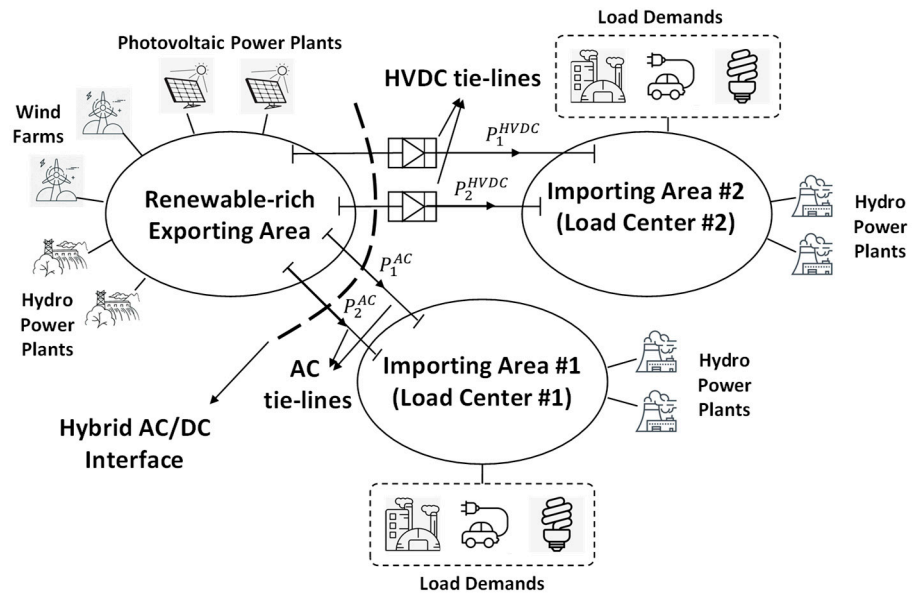


Figure 1. Demonstration of renewable-rich power grid with hybrid AC/DC interface.

Total transfer capacity (TTC) [14] evaluates the maximum allowable power flow that can be transferred through a critical interface of the transmission network without the violation of some specific stability constraints, such as thermal limits, voltage stability limits and transient stability limits [15]. The TTC of an interface is highly dependent on the network structure. On the other hand, the TTC can be used to indicate the effectiveness of the planned network structure. In this section, the mathematical modeling and the computation of the TTC of hybrid AC/DC interface are discussed.

2.1. Mathematical Modeling

Mathematically, TTC of a transmission interface can be formulated as an extended optimal power flow problem that searches for the worst-case operating condition which are located on the security boundary. In this paper, the optimization model for transfer capacity of hybrid AC/DC interface is proposed as follows.

2.1.1. Objective Function

The objective function for TTC computation is given in (1):

$$\min \left\{ \begin{array}{l} P_i^G, i \in G \\ P_{ij}^{DC}, \langle i, j \rangle \in I_{DC} \end{array} \right\} \left(\sum_{\langle i, j \rangle \in I_{AC}} P_{ij}^{AC} + \sum_{\langle i, j \rangle \in I_{DC}} P_{ij}^{DC} \right) \quad (1)$$

where I_{AC} and I_{DC} are the set of AC tie-lines and the set of HVDC tie-lines that together form the hybrid transmission interface. P_{ij}^{AC} denotes the active power flow through the AC tie-line from Bus i to Bus j , while P_{ij}^{DC} denotes the transferred active power through the DC tie-line. In this optimization problem, the decision variables include the active power generation P_i^G of all the power plants and the active power P_{ij}^{DC} of all the DC tie-lines.

2.1.2. Power Flow Equation Constraints

The AC power flow equation constraints are given in (2) and (3):

$$P_{G,i} - P_{D,i} - P_{HVDC,i} = V_i \sum_{j=1}^{N_S} V_j (G_{ij} \cos \theta_{ij} + B_{ij} \sin \theta_{ij}) \quad (2)$$

$$Q_{G,i} - Q_{D,i} - Q_{HVDC,i} = V_i \sum_{j=1}^n V_j (G_{ij} \sin \theta_{ij} - B_{ij} \cos \theta_{ij}) \quad (3)$$

where $P_{G,i}$ is the injected real power at bus i from the generator and $P_{G,i} = 0$ if there is no generator connected to bus i . $P_{D,i}$ is the real power consumption at bus i . $P_{HVDC,i}$ is the real power absorbed by the converter of the related HVDC tie-line and $P_{HVDC,i} = 0$ if there is no HVDC tie-line connected to bus i . $Q_{G,i}$, $Q_{D,i}$ and $Q_{HVDC,i}$ are the related reactive power values. V_i and V_j are the bus voltage magnitude of bus i and bus j . G_{ij} and B_{ij} are the real and image parts of the related element in the nodal admittance matrix. $\theta_{ij} = \theta_i - \theta_j$ is the difference of voltage phase angle between bus i and bus j .

2.1.3. Steady State Security Constraints

For the computed worst-case operating condition that is related with the TTC computation, the steady state security constraints, such as the branch loading constraint and the bus voltage security constraint, should be satisfied. They are given in (4) and (5):

$$|S_{ij}| \leq S_{ij}^{max}, \langle i, j \rangle \in L_{AC} \quad (4)$$

$$V_i^{min} \leq V_i \leq V_i^{max}, i \in B \quad (5)$$

where $|S_{ij}|$ is the complex power that is transmitted through the AC transmission line from bus i to bus j , while S_{ij}^{max} is the maximum value determined by its thermal limit. V_i^{min} and V_i^{max} are the lower and upper limit of bus voltage magnitude.

2.1.4. Differential Algebraic Equations (DAEs)-Based Dynamic Security Constraints

Dynamic security constraints are given in (6)–(9):

$$\dot{x} = F(x, y, c) \quad (6)$$

$$0 = G(x, y, c) \quad (7)$$

$$\varphi_{TSA}(x, y, c) \geq 0 \quad (8)$$

$$c \in C_{AC} \cup C_{DC} \quad (9)$$

where f denotes the differential equations, g denotes the algebraic equations, x denotes the state variable relating to dynamic components, such as generators and their automatic voltage regulators and turbine governors, y denotes the algebraic variable including bus voltage and power flow on transmission lines, u denotes the controllable input variable, and c refers to a specific fault contingency. C_{AC} and C_{DC} denote the fault contingencies related to AC tie-lines and HVDC tie-lines, respectively. φ_{TSA} denotes a specific transient stability assessment criterion and the single machine equivalent (SIME) method is used.

2.1.5. Security Boundary-Oriented Constraint

As is discussed, the computation of TTC is to search for the worst-case operating condition which are located on the security boundary. In this paper, the security boundary is determined jointly by the dynamic security and the steady state thermal security. This constraint is enabled by (10):

$$\min\{\varphi_{TSA}, \varphi_{Thermal}\} = 0 \quad (10)$$

where

$$\varphi_{Thermal} = \min_{\langle i,j \rangle \in L_{AC}} \left(S_{ij}^{max} - |S_{ij}| \right) \quad (11)$$

$\varphi_{Thermal}$ denotes the thermal security criterion of AC transmission lines. Equation (10) ensures that the solution should be located on the security boundary which is determined by either the transient stability or the thermal security.

2.1.6. Feasible Constraints of Decision Variables

The decision variables include the active power generation P_i^G of all the power plants and the active power P_{ij}^{DC} of all the DC tie-lines. The feasible constraints of these variables are given respectively in (12) and (13):

$$P_i^{G,min} \leq P_i^G \leq P_i^{G,max}, i \in G \quad (12)$$

$$P_{ij}^{DC,min} \leq P_{ij}^{DC} \leq P_{ij}^{DC,max}, \langle i,j \rangle \in I_{DC} \quad (13)$$

where $P_i^{G,min}$ and $P_i^{G,max}$ are the lower and upper limit of the active power generation for the i th power plant. $P_{ij}^{DC,min}$ and $P_{ij}^{DC,max}$ are the lower and upper limit of HVDC tie-lines.

2.2. Heuristic Method for Transfer Capacity Computation

As is shown in (1)–(13), the optimization model for transfer capacity computation is a complex dynamic programming problem. Conventional approaches transform this model into a nonlinear optimization model by the discretization of the DAEs. However, when the number of contingencies increases, the number of nonlinear equality constraints also increase significantly. It makes it very challenging to solve this nonlinear optimization problem for a practical large-scale power network. In this section, a heuristic method is proposed as the alternative. The procedure of the proposed heuristic method is introduced as follows.

- Step 1: Determine the critical hybrid AC/DC interface that is of interest. With the HVDC bi-pole blocking scenario as the large disturbance contingency, the post-disturbance response of the power system is obtained by time-domain simulation (TDS). Then, the critical AC cut-set can be identified by the branch potential energy function criterion [16]. The HVDC tie-line and the AC cut-set together form the critical hybrid AC/DC interface;
- Step 2: Determine the base operating condition. The load demand is firstly determined by long-term load forecasting. With the given network structure, the generation of each power plant can be computed by conventional economic dispatch algorithm. The solution of the economic dispatch is used as the base operating condition;
- Step 3: Perform contingency analysis. The credible contingencies are pre-determined based on the experience of transmission system operators (TSOs) or generated by considering the typical fault contingencies, such as short-circuit faults of AC transmission lines and HVDC bi-pole blocking. All the contingencies are simulated and the stability margin φ_{TSA}^{base} is assessed. If security margin is less than a given threshold, go to Step 6; otherwise, proceed to the next step;
- Step 4: Compute the sensitivities of decision variables to the stability margin. Instead of the analytical trajectory sensitivity [17], the numerical sensitivity is computed in consideration that the Jacobian matrix of the DAEs is usually not available for commercial power system analysis software; meanwhile, real-time decision making is not the prior concern for TEP problem. With N_d decision variables, N_d times of time-domain simulation is carried out in order to assess the changed stability margin under small perturbation of each variable. Then, the sensitivity can be computed by (14):

$$\frac{d\varphi_{TSA}(x,y,c,u)}{du} \approx \frac{\varphi_{TSA}(x,y,c,u + \Delta u) - \varphi_{TSA}(x,y,c,u)}{\Delta u} \quad (14)$$

where $u \in \{P_i^G, i \in G\} \cup \{P_{ij}^{DC}, \langle i, j \rangle \in I_{DC}\}$;

- Step 5: Compute the linearized optimization model. Based on the sensitivities to the stability margin and the DC power flow model, the linearized optimization model is derived as follows.

$$\min_{\left\{ \begin{array}{l} \Delta P_i^G, i \in G \\ \Delta P_{ij}^{DC}, \langle i, j \rangle \in I_{DC} \end{array} \right\}} \left(\sum_{\langle i, j \rangle \in I_{AC}} P_{ij}^{AC} + \sum_{\langle i, j \rangle \in I_{DC}} P_{ij}^{DC} \right) \tag{15}$$

$$\text{s.t.} \left\{ \begin{array}{l} \varphi_{TSA}^{base} + \sum_{i \in G} \frac{d\varphi_{TSA}(x, y, c, P_i^G)}{dP_i^G} \Delta P_i^G + \sum_{i \in G} \frac{d\varphi_{TSA}(x, y, c, P_{ij}^{DC})}{dP_{ij}^{DC}} \Delta P_{ij}^{DC} = 0 \\ P_i^G + \Delta P_i^G - P_{D,i} - P_{ij}^{DC} - \Delta P_{ij}^{DC} = B\theta \\ |P_{ij}| \leq S_{ij}^{max}, \langle i, j \rangle \in L_{AC} \\ P_i^{G, min} \leq P_i^G + \Delta P_i^G \leq P_i^{G, max}, i \in G \\ P_{ij}^{DC, min} \leq P_{ij}^{DC} + \Delta P_{ij}^{DC} \leq P_{ij}^{DC, max}, \langle i, j \rangle \in I_{DC} \end{array} \right. \tag{16}$$

where B is the nodal admittance matrix for DC power flow and $\theta = [\theta_1 \cdots \theta_{N_B}]^T$. By computing the linearized optimization model in (15–16), the increment or decrement of the decision variables can be computed and then the operating condition is updated by (17) and (18):

$$P_i^G \leftarrow P_i^G + \Delta P_i^G \tag{17}$$

$$P_{ij}^{DC} \leftarrow P_{ij}^{DC} + \Delta P_{ij}^{DC} \tag{18}$$

Then, go back to Step 3;

- Step 6: The critical operating condition is obtained and the transfer limit of the hybrid AC/DC interface is also determined, which will be used as the transfer limits of the hybrid AC/DC interface during the optimization of TEP so as to account for the dynamic security of the system.

3. The Proposed Multi-Period Transmission Expansion Planning Scheme

3.1. The Optimization Model

Assuming that the planning schemes of generation expansion planning (GEP) and the HVDC integration are determined beforehand, the proposed multi-period transmission expansion planning model attempts to reinforce the AC transmission network in order to maximize the TTC of the hybrid interface during each stage of the planning horizon.

3.1.1. Objectives

The objective of the proposed TEP model is two-fold, including the minimization of investment cost f_1 and the minimization of the aggregated cost of operation and renewable curtailment f_2 :

$$\min\{f_1, f_2\} \tag{19}$$

$$f_1 = \min \sum_{t \in T} \left[\frac{\sum_{i, j \in \Omega^+} c_{ij} (n_{ij,t} - n_{ij,t-1})}{(1+r)^{t-1}} \right] \tag{20}$$

$$f_2 = \min \sum_{t \in T} \left[\frac{\sum_{g \in G} c_g P_{g,t}^G + \sum_{g \in G^E} c_g^{curtailment} (P_{g,t}^{G, max} - P_{g,t}^G)}{(1+r)^{t-1}} \right] \tag{21}$$

where T is the number of planning years and t indicates a specific year during the planning horizon. Ω^+ denotes the set of transmission lines that can be constructed. c_{ij} is the investment cost for the candidate AC transmission line $\langle i, j \rangle$, while $n_{ij,t}$ is a binary variable that indicates whether the related transmission line has been constructed and is put into operation at year t . c_g is the cost coefficient for the g th generator and $P_{g,t}^G$ is the generation

dispatch at year t . G^E denotes the subset of generators that locate at the energy-exporting area. $c_g^{curtailment}$ is the cost coefficient for renewable curtailment and $P_{g,t}^{G,max}$ is the maximum available generation for the g th generator. r is the discount rate for long-term investment.

3.1.2. Power Flow and Steady State Security Constraints for Normal and N-1 Scenarios

At each stage, the power flow and steady state security constraints should be satisfied for both normal and N-1 scenarios:

$$P_t^G - P_t^{DC} - P_t^D = B_t^{N-0} \theta_t, \forall t \quad (22)$$

$$|P_{ij,t}^{N-0}| \leq n_{ij,t} S_{ij}^{max}, \forall t, \langle i, j \rangle \in L_{AC} \quad (23)$$

$$P_t^G - P_t^{DC} - P_t^D = B_t^{N-1} \theta_t, \forall t \quad (24)$$

$$|P_{ij,t}^{N-1}| \leq n_{ij,t} S_{ij}^{max}, \forall t, \langle i, j \rangle \in L_{AC} \quad (25)$$

where P_t^G , P_t^{DC} and P_t^D are the vectors of real power generation, power exchange with HVDC tie-lines, and load demand for all the AC buses. B_t is the nodal admittance matrix for DC power flow computation and θ_t denotes the vector of bus voltage phase. The superscripts of N-0 and N-1, respectively, indicate the normal and N-1 scenarios. $P_{ij,t}^{N-0}$ and $P_{ij,t}^{N-1}$ are the real power flow through the AC transmission line from bus i to bus j under different scenarios.

3.1.3. Security Constraint for Hybrid AC/DC Interface

Apart from the above mentioned steady state security constraints, the dynamic security constraint for hybrid AC/DC interface should also be satisfied:

$$\sum_{\langle i,j \rangle \in I_{AC}} P_{ij,t}^{AC} + \sum_{\langle i,j \rangle \in I_{DC}} P_{ij,t}^{DC} \leq P_t^{TTC} \quad (26)$$

where P_t^{TTC} is the total transfer capacity of the hybrid AC/DC interface at year t under the given planned network structure. P_t^{TTC} is computed by the heuristic method proposed in Section 2.2.

3.1.4. Feasibility Constraints for Decision Variables

The decision variables for the proposed multi-stage TEP model includes the TEP strategy that is related with the transmission lines to be built at different stages and is represented by the binary variables $n_{ij,t}$ and meanwhile the continuous variables that is related with the operating conditions at different stages. The feasibility constraints for decision variables are given in (27)–(30):

$$P_{g,t}^{G,min} \leq P_{g,t}^G \leq P_{g,t}^{G,max}, \forall t, g \in G \quad (27)$$

$$P_{ij,t}^{DC,min} \leq P_{ij,t}^{DC} \leq P_{ij,t}^{DC,max}, \forall t, \langle i, j \rangle \in I_{DC} \quad (28)$$

$$n_{ij}^{min} \leq n_{ij,t} \leq n_{ij}^{max}, \forall t \quad (29)$$

$$n_{ij,t-1} \leq n_{ij,t}, \forall t \quad (30)$$

where n_{ij}^{min} and n_{ij}^{max} are the minimum and maximum number of parallel transmission lines that can be built.

3.2. The Solution Methodology

Considering that this TEP model is a multi-objective optimization model with nonlinear constraints and integer variables, the well-established non-dominated sorting genetic algorithm-II (NSGA-II) [18] is used to compute the optimal solution. The solution methodology is introduced as follows.

3.2.1. Encoding and Initialization of the Population

For the multi-objective optimization model in (19)–(30), the decision variables include the integer variables $n_{ij,t}$ and the continuous variables $P_{g,t}^G$ and $P_{ij,t}^{DC}$. However, these continuous variables are strongly dependent on the integer variables; in other words, the network structure under a given transmission expansion scheme. Therefore, this paper treats these variables in a manner similar to bi-level optimization. The population is characterized only by the integer variables. Considering that the integer variables $n_{ij,t}$ denote the number of parallel transmission lines through any corridors, integer variables $n_{ij,t}$ are encoded based on the binary system and then are concatenated based on the pre-defined order of transmission corridors. Instead of explicitly optimizing the continuous variables during the process of evolution, they are computed by the subproblem. Based on the above-mentioned scheme for encoding, the population is initialized independently by binary random sampling.

3.2.2. Fitness Evaluation

Defining the transmission expansion scheme based on a given individual of the population, the network structures for all the stages are determined. The procedure for fitness evaluation is proposed as follows.

- Step 1: compute the optimal value of the continuous variables $P_{g,t}^G$ based on the DC optimal power flow defined by (22)–(25) and (27);
- Step 2: with the solution of the continuous variables $P_{g,t}^G$ to be the initial guess of the problem in (1)–(13), compute the total transfer capacity P_t^{TTC} of the hybrid AC/DC interface based on the proposed heuristic method in Section 2.2;
- Step 3: again, compute the optimal value of the continuous variables $P_{g,t}^G$ and $P_{ij,t}^{DC}$ based on the extended DC optimal power flow defined by (22)–(28);
- Step 4: based on the solution of the former step, compute the investment cost, the operation cost and the transfer capacity as in (20) and (21);
- Step 5: then, the computed values of the objective functions are used as the indicator of fitness of any individuals.

3.2.3. The Procedure of Computation of the TEP Scheme Based on NSGA-II

The procedure of evolution-based optimization for a transmission expansion planning scheme is the same as the standard NSGA-II, which includes the crossover, the mutation and more importantly the non-dominated sorting. The technical details of NSGA-II can be found in [18] and are not introduced here due to the limit of space. The flowchart of the procedure is shown in Figure 2. The technical details of each step are discussed as follows:

- Step 1: determine the inputs and constraints of multi-period transmission expansion planning problem, including the initial network structure of the power grid, the annual increasing ratio of load demands, the long-term generation expansion planning scheme and the HVDC integration planning scheme;
- Step 2: Initialize the iteration coefficient $l = 0$. Set the maximum iteration M (for example, $M = 100$). Set the size of population N ($N = 100$ in this paper);

- Step 3: initialize the parent population NP_i ($I = 0$) based on randomized binary sampling on the encoding of the TEP schemes;
- Step 4: Generate the offspring population NQ_i with size N from the parent population NP_i through crossover and mutation. Check all the individuals in the offspring population NQ_i . If there are any violations of the decision variables constraints in (29) and (30), adjust the encoding of the related individuals so that the constraints in (29) and (30) are always satisfied;
- Step 5: combine NP_i and NQ_i to form the population K_i with the size of $2N$. Evaluate the fitness of the population K_i according to the procedure discussed in Section 3.2.2;
- Step 6: perform the non-dominated sorting to divide K_i into several non-dominated layers (F_1, F_2, \dots, F_L);
- Step 7: Following the sequence of the non-dominated layers (F_1, F_2, \dots, F_L), the individuals of each non-dominated layer F_l are added to a new population NP_{i+1} until the size of NP_{i+1} is equal to N . The rest of the individuals in F_{l+1} and later layers are eliminated;
- Step 8: If the maximum iteration is reached, i.e., $i \geq M$, go to Step 9. Otherwise, let $i = i + 1$ and go back to Step 4;
- Step 9: check the solutions in the first non-dominated layer F_1 , the solution that has the lowest investment cost and will not result in renewable curtailments is selected as the final transmission expansion planning scheme.

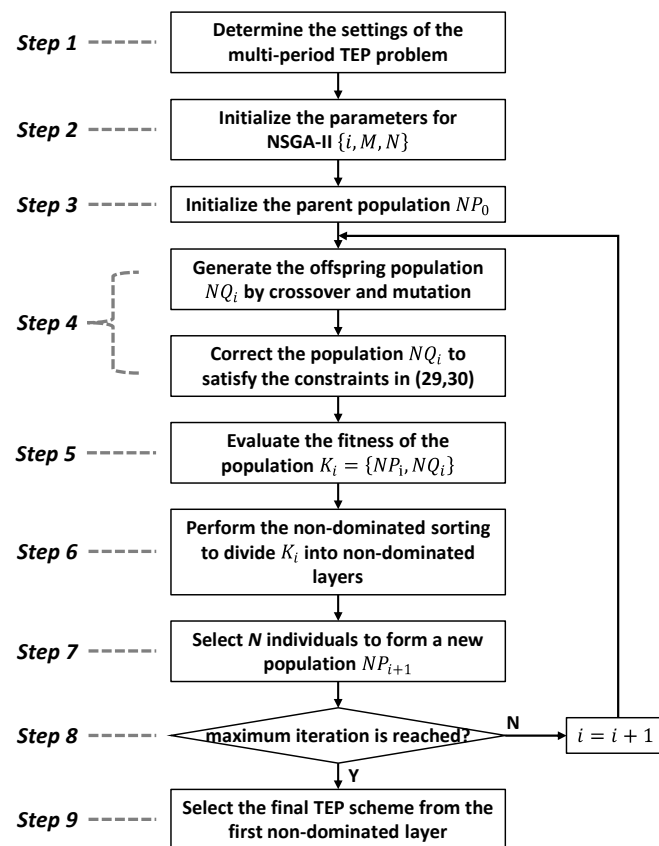


Figure 2. Flowchart of the procedure of computation of the TEP scheme based on NSGA-II.

4. Results

4.1. Testing System

This case study is carried out by using a modified IEEE 10-machine 39-bus system, whose network structure is shown in Figure 2. The model data of the original IEEE 10-machine 39-bus system can be found on [19]. At the initial stage, Bus-(20,21,22,34,35) are removed from the network, which simulates that these substations and the relating transmission line are not constructed. In this modified testing system, two HVDC tie-lines are planned to be connected to Bus-19 and Bus-22 and their rated power are both 4000MW. So, the hybrid interface is composed of these two HVDC tie-lines and the AC transmission lines 15–16 and 16–17. The synchronous generator at Bus-34 is replaced by a double-fed induction generator (DFIG)-based wind farm with the capacity of 2400 MW. Additionally, the synchronous generators at Bus-(33,35,36) are considered as hydro generators and their rated capacity are increased to 2400 MW to represent the results of generation expansion planning. The overall planning horizon for multi-period TEP is set to be 5 years and each period is 1 year. The load demand in the energy-importing area increases by 10% each year. For each transmission corridor, the maximum number of transmission lines that can be built is set to be 4. The length of transmission lines is assumed to be proportional to the reactance by the ratio of 1mile/0.001p.u. and the investment cost is CNY 100 thousand/mile. The electricity price for thermal, hydro and wind power are CNY 50/MWh, CNY 20/MWh and CNY 10/MWh.

4.2. TEP Based on the Proposed Model

The HVDC tie-lines are scheduled to be put into operation in the second and the fifth year, respectively. Based on the proposed model, the transmission expansion planning scheme is computed and the numerical results are shown in Table 1. Nineteen transmission lines and two transformers are built during the five year planning and the aggregated investment cost is CNY 29,633.9. The branches that are put into operation in each planning year can be seen in Figure 3. It should be noted that the dotted line in Figure 3 is used to highlight the additional branches under the proposed model for better comparison with the conventional model (which will be discussed in Section 4.3 in detail).

Table 1. The multi-period planning scheme based on the proposed model (Scheme 1).

Stage	HVDC Tie-lines	Generation Units	Investment Cost/Thousand	Operation Cost/Thousand	Curtailment of Renewable Generation/MW
1	\	G33-2	CNY 3780.0	CNY 15,960	250.0
2	HVDC-19	W34-1/W34-2 W34-3/W34-4 G33-3\G33-4	CNY 2419.1	CNY 22,227.2	0.0
3	\	G35-1	CNY 5514.7	CNY 20,836.1	0.0
4	\	W24	CNY 12,560.2	CNY 19,384.5	0.0
5	HVDC-22	G35-2\G35-3 G35-4 G36-2\G36-3 G35-4	5359.9	28,429.8	100.0

4.3. Comparison with Conventional TEP Model

To further demonstrate the effectiveness of the proposed model is a comparative case study with a conventional adequacy model, i.e., the model without considering the dynamic security of the hybrid AC\DC interface. The planning scheme of the conventional adequacy model is shown in Figure 4, while the numerical results on investment cost, operation cost and renewable curtailment are provided in Table 2.

Table 2. The multi-period planning scheme based on the conventional model (Scheme 2).

Stage	Newly Constructed Branches	Investment Cost/Thousand	Operation Cost/Thousand	Curtailment of Renewable Generation/MW
1	<16-19-2>	CNY 1950.0	CNY 17,204.1	800.0
2	<19-20-1> <19-20-2> <19-20-3> <20-34>	CNY 2419.1	CNY 23,421.2	400.0
3	<16-21-1> <21-22-1> <22-23-1> <22-25>	CNY 4662.1	CNY 23,317.8	1100.0
4	/	CNY 0.0	CNY 21,639.6	1312.5
5	<1-2-2> <1-39-2> <8-9-2> <9-39-2> <16-24-2> <22-23-2> <22-23-3>	CNY 2982.3	CNY 31,285.3	1071.0

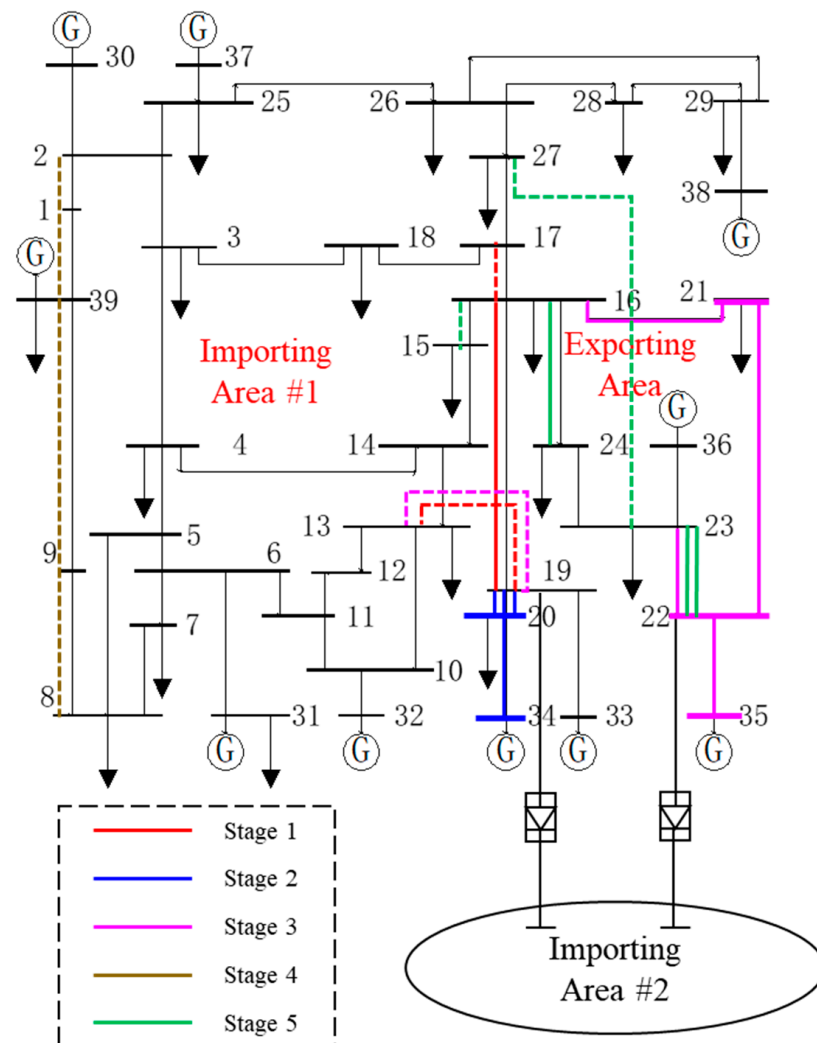


Figure 3. The network structure of the modified IEEE 39-bus system.

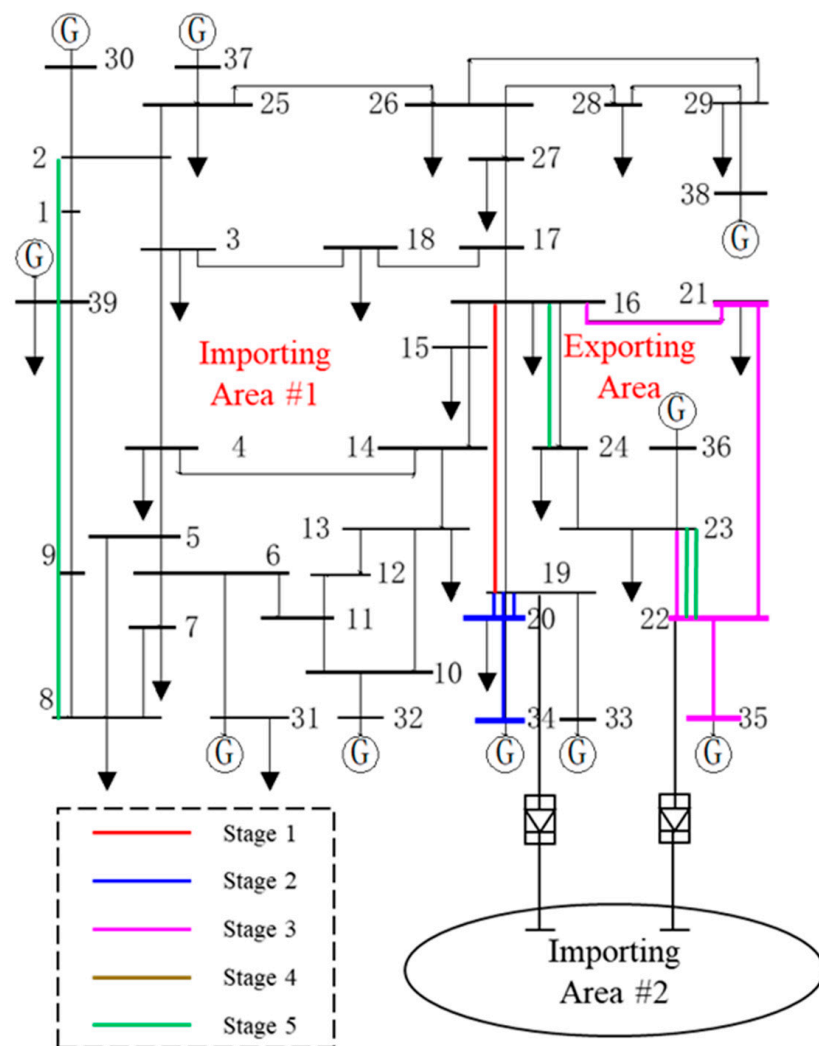


Figure 4. The transmission expansion planning scheme under the conventional model.

As more transmission lines are constructed, the investment cost under Scheme 1 is higher than the investment cost under Scheme 2 (CNY 12,013.5). However, in each planning year, the operation cost under Scheme 1 is lower than the operation cost under Scheme 2. This is because, as more branches have been built and thus the AC power grid is significantly strengthened, the transfer capacity of the hybrid AC/DC interface under Scheme 1 is higher. Then, as a result, the curtailment of renewables in the energy-exporting area decreases, which in turn reduces the holistic electricity purchasing price and the curtailment cost.

To further demonstrate that the proposed model can enhance the dynamic security and also the total transfer capacity of the hybrid AC/DC interface in comparison with the conventional model, a time-domain simulation-based contingency analysis is carried out. The post-contingency rotor angle trajectories are shown in Figure 5.

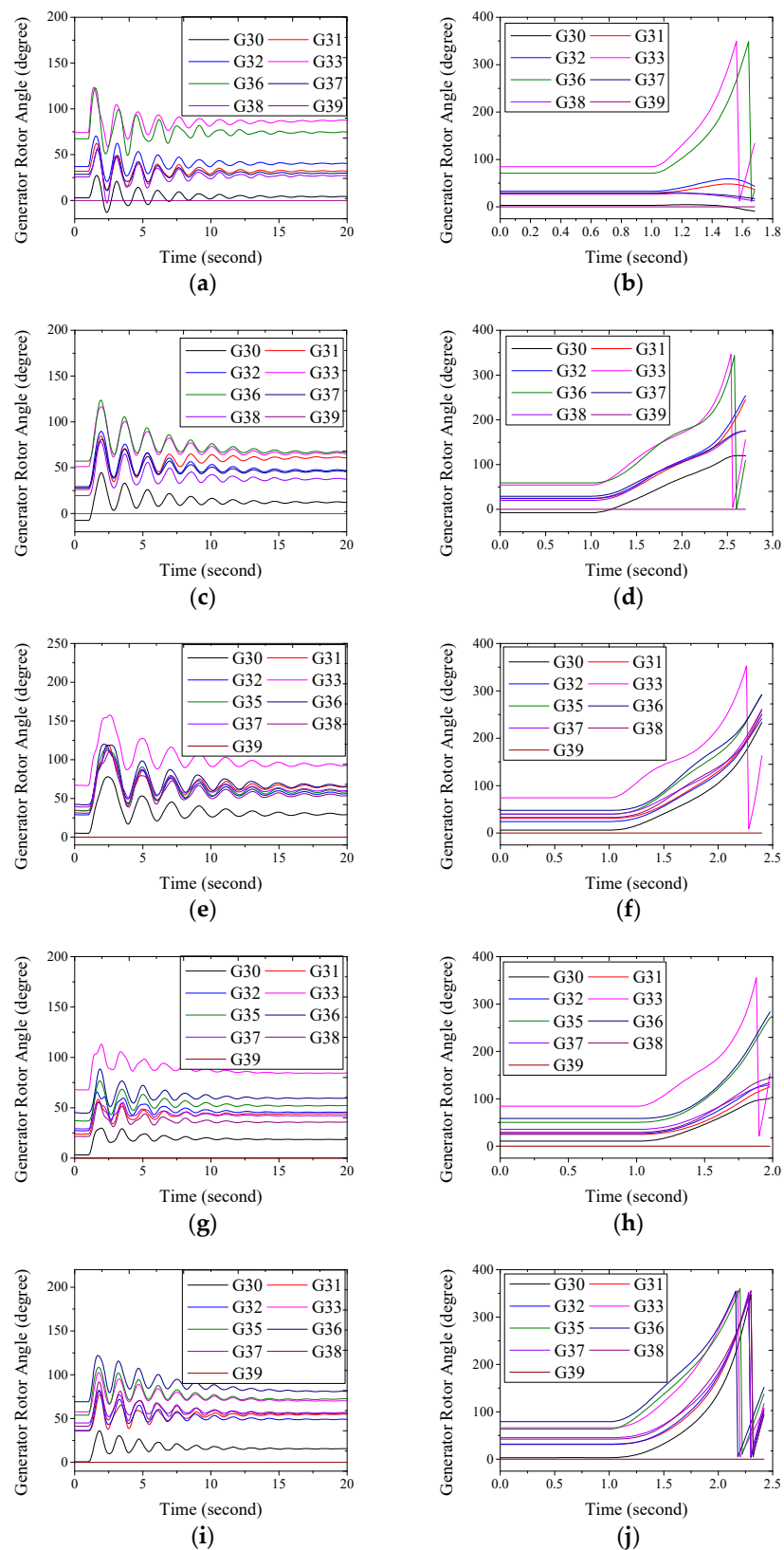


Figure 5. The post-contingency trajectories under different planning schemes. (a) Stage 1 under Scheme 1. (b) Stage 1 under Scheme 2. (c) Stage 2 under Scheme 1. (d) Stage 2 under Scheme 2. (e) Stage 3 under Scheme 1. (f) Stage 3 under Scheme 2. (g) Stage 4 under Scheme 1. (h) Stage 4 under Scheme 2. (i) Stage 5 under Scheme 1. (j) Stage 5 under Scheme 2.

It can be seen that, when the same amount of active power flow is transmitted through the hybrid AC/DC interface, the power grid of Scheme 1 is able to withstand the critical contingency, while the power grid of Scheme 2 will lose its stability after the occurrence of the contingency. To prevent the power grid of Scheme 2 from dynamic insecurity, the active power flow should be reduced, which inevitably results in the curtailment of renewable generations.

5. Conclusions

With the increasing integration of HVDC tie-lines, the regional power systems in both the energy-exporting area and the energy-importing area have been gradually evolving into “strong DC, weak AC” systems. In this paper, a multi-period transmission expansion planning optimization model is proposed for energy-exporting area with hybrid AC/DC interface. While the existing literature has not considered the dynamic security problem in TEP, this paper adopts the conventional total transfer capacity (TTC) index to evaluate the security limit of hybrid AC/DC interface under different transmission expansion schemes. Multiple objectives are considered to reduce the investment cost while minimizing the curtailment of renewables due to the inadequate transfer capacity of the interface. Case study on the modified IEEE 39-bus system is presented to demonstrate the effectiveness of the proposed method. Numerical results show that the proposed model can maximize the total transfer capacity of the hybrid AC/DC interface so as to promote the consumption of renewables, while the conventional model cannot guarantee the dynamic security and therefore results in renewable curtailments.

Author Contributions: Conceptualization, L.S.; methodology, L.J.; software, Q.W.; validation, Y.W. and T.L.; writing—original draft preparation, L.S.; writing—review and editing, T.L.; All authors have read and agreed to the published version of the manuscript.

Funding: This work is supported by the science and technology project of State Grid Southwest Branch Corporation (Grant No.: 52999820000W).

Data Availability Statement: Not applicable.

Conflicts of Interest: The authors declare no conflict of interest. The funders had no role in the design of the study; in the collection, analyses, or interpretation of data; in the writing of the manuscript; or in the decision to publish the results.

References

1. Padiyar, K.R. *HVDC Power Transmission*; Wiley: New York, NY, USA, 1990.
2. Wang, Q.; Li, T.; Yang, P. Analysis of impact of “strong DC and weak AC” on receiving-end power system. *IOP Conf. Ser. Earth Environ. Sci.* **2018**, *113*, 1–7. [[CrossRef](#)]
3. Zhao, T.; Liu, Y.; Xie, H.; Zi, P.; Wang, Z.; Lu, W. Mechanism Analysis on Transient Stability of the Weak Sending-end System Considering Dynamic Characteristics of HVDC. In Proceedings of the 2021 International Conference on Power System Technology (POWERCON), Haikou, China, 8–9 December 2021; pp. 1438–1442.
4. Wang, W.; Xiong, X.; Li, M.; Yu, R. A Flexible Control Strategy to Prevent Sending-End Power System From Transient Instability Under HVDC Repetitive Failures. *IEEE Trans. Power Syst.* **2020**, *35*, 4445–4458. [[CrossRef](#)]
5. Zhou, B.; Fang, J.; Ai, X.; Yang, C.; Yao, W.; Wen, J. Dynamic Var Reserve-Constrained Coordinated Scheduling of LCC-HVDC Receiving-End System Considering Contingencies and Wind Uncertainties. *IEEE Trans. Sustain. Energy* **2021**, *12*, 469–481. [[CrossRef](#)]
6. Yang, D.; Zhao, K.; Liu, Y. Coordinated optimization for controlling short circuit current and multi-infeed DC interaction. *Mod. Power Syst. Clean Energy* **2014**, *2*, 274–284. [[CrossRef](#)]
7. Lotfjou, A.; Fu, Y.; Shahidepour, M. Hybrid AC/DC Transmission Expansion Planning. *IEEE Trans. Power Deliv.* **2012**, *27*, 620–628. [[CrossRef](#)]
8. Zhang, X.; Tomsovic, K.; Dimitrovski, A. Security Constrained Multi-Stage Transmission Expansion Planning Considering a Continuously Variable Series Reactor. *IEEE Trans. Power Syst.* **2017**, *32*, 4442–4450. [[CrossRef](#)]
9. Moradi-Sepahvand, M.; Amraee, T. Hybrid AC/DC Transmission Expansion Planning Considering HVAC to HVDC Conversion Under Renewable Penetration. *IEEE Trans. Power Syst.* **2020**, *36*, 579–591. [[CrossRef](#)]
10. Bhattiprolu, P.A.; Conejo, A.J. Multi-Period AC/DC Transmission Expansion Planning Including Shunt Compensation. *IEEE Trans. Power Syst.* **2021**, *37*, 2164–2176. [[CrossRef](#)]

11. Wen, Y.; Lu, Y.; Gou, J.; Liu, F.; Tang, Q.; Wang, R. Robust Transmission Expansion Planning of Ultrahigh-Voltage AC–DC Hybrid Grids. *IEEE Trans. Ind. Appl.* **2022**, *58*, 3294–3302. [[CrossRef](#)]
12. Barati, F.; Seifi, H.; Sepasian, M.S.; Nateghi, A.; Shafie-khah, M.; Catalão, J.P.S. Multi-Period Integrated Framework of Generation, Transmission, and Natural Gas Grid Expansion Planning for Large-Scale Systems. *IEEE Trans. Power Syst.* **2014**, *30*, 2527–2537. [[CrossRef](#)]
13. Shen, L.; Jiang, L.; Wang, Q.; Wen, Y.; Liu, T.; Liu, H. Bi-Level Transmission Expansion Planning Considering The Transfer Capacity of Hybrid AC/DC Interface. In Proceedings of the 2022 4th International Conference on Electrical Engineering and Control Technologies (CEECT), Shanghai, China, 16–18 December 2022; pp. 396–400. [[CrossRef](#)]
14. NERC. *Available Transfer Capability Definition and Determination*; North America Electric Reliability Council: Washington, DC, USA, 1996.
15. Hou, G.; Vittal, V. Determination of Transient Stability Constrained Interface Real Power Flow Limit Using Trajectory Sensitivity Approach. *IEEE Trans. Power Syst.* **2013**, *28*, 2156–2163. [[CrossRef](#)]
16. Padiyar, K.R.; Krishna, S. Online detection of loss of synchronism using energy function criterion. *IEEE Trans. Power Deliv.* **2006**, *21*, 46–55. [[CrossRef](#)]
17. Hiskens, I.A.; Pai, M.A. Trajectory sensitivity analysis of hybrid systems. *IEEE Trans. Circuits Syst. I Fundam. Theory Appl.* **2000**, *47*, 204–220. [[CrossRef](#)]
18. Deb, K.; Pratap, A.; Agarwal, S.; Meyarivan, T. A fast and elitist multiobjective genetic algorithm: NSGA-II. *IEEE Trans. Evol. Comput.* **2002**, *6*, 182–197. [[CrossRef](#)]
19. Power Systems Test Case Archive. Available online: <http://labs.ece.uw.edu/pstca/> (accessed on 28 December 2022).

Disclaimer/Publisher’s Note: The statements, opinions and data contained in all publications are solely those of the individual author(s) and contributor(s) and not of MDPI and/or the editor(s). MDPI and/or the editor(s) disclaim responsibility for any injury to people or property resulting from any ideas, methods, instructions or products referred to in the content.